Inorg. Chem. **2003**, *42*, 844–850

Inorganic Chemistry
Article

Subtle Role of Polyatomic Anions in Molecular Construction: Structures and Properties of AgX Bearing 2,4′-Thiobis(pyridine) ($X^- = NO_3^-$, BF_4^-, ClO_4^-, PF_6^-, $CF_3CO_2^-$, and $CF_3SO_3^-$)

Ok-Sang Jung,[*,†] Yun Ju Kim,[†] Young-A Lee,[†] Ki-Min Park,[‡] and Shim Sung Lee[‡]

Materials Chemistry Laboratory, Korea Institute of Science and Technology, Seoul 136-791, Korea, and Department of Chemistry and Research Institute of Natural Science, Gyeongsang National University, Chinju 660-701, Korea

Received August 8, 2002

Studies on the subtle effects and roles of polyatomic anions in the self-assembly of a series of AgX complexes with 2,4′-Py_2S ($X^- = NO_3^-$, BF_4^-, ClO_4^-, PF_6^-, $CF_3CO_2^-$, and $CF_3SO_3^-$; 2,4′-Py_2S = 2,4′-thiobis(pyridine)) have been carried out. The formation of products appears to be primarily associated with a suitable combination of the skewed conformers of 2,4′-Py_2S and a variety of coordination geometries of Ag(I) ions. The molecular construction via self-assembly is delicately dependent upon the nature of the anions. Coordinating anions afford the 1:1 adducts [Ag(2,4′-Py_2S)X] ($X^- = NO_3^-$ and $CF_3CO_2^-$), whereas noncoordinating anions form the 3:4 adducts [Ag_3(2,4′-$Py_2S)_4$]X_3 ($X^- = ClO_4^-$ and PF_6^-). Each structure seems to be constructed by competition between π–π interactions of 2,4′-Py_2S spacers vs Ag···X interactions. For ClO_4^- and PF_6^-, an anion-free network consisting of linear Ag(I) and trigonal Ag(I) in a 1:2 ratio has been obtained whereas, for the coordinating anions NO_3^- and $CF_3CO_2^-$, an anion-bridged helix sheet and an anion-bridged cyclic dimer chain, respectively, have been assembled. For a moderately coordinating anion, $CF_3SO_3^-$, the 3:4 adduct [Ag_3(2,4′-$Py_2S)_4$]($CF_3SO_3)_3$ has been obtained similarly to the noncoordinating anions, but its structure is a double strand via both face-to-face (π–π) stackings and Ag···Ag interactions, in contrast to the noncoordinating anions. The anion exchanges of [Ag_3(2,4′-$Py_2S)_4$]X_3 ($X^- = BF_4^-$, ClO_4^-, and PF_6^-) with BF_4^-, ClO_4^-, and PF_6^- in aqueous media indicate that a [BF_4^-] analogue is isostructural with [Ag_3(2,4′-$Py_2S)_4$]X_3 ($X^- = ClO_4^-$ and PF_6^-). Furthermore, the anion exchangeability for the noncoordinating anion compounds and the X-ray data for the coordinating anion compounds establish the coordinating order to be $NO_3^- > CF_3CO_2^- > CF_3SO_3^- > PF_6^- > ClO_4^- > BF_4^-$.

Introduction

Various intriguing molecular frames have been designed and assembled by the selection of basic components such as the coordination geometry of metal ions, the binding site of donating atoms, and the length of spacers or/and by the induction of weak intra- or intermolecular interactions.[1−10] Rational control of molecular frameworks via (counter)anions is rare due to the less effective electrostatic binding interactions.[11] Recently, however, anion coordination chemistry has become a rapidly emerging field owing to a timely interest from environmental pollution, industrial chemical, biological process, ionic liquids, catalysis, lithium battery, and health-related perspectives.[12−18] More recent developments include exciting advances in anion template assembly, ion-pair

---

* To whom correspondence should be addressed. E-mail: oksjung@kist.re.kr.

[†] Korea Institute of Science and Technology.

[‡] Gyeongsang National University.

(1) Stang, P. J.; Olenyuk, B. *Acc. Chem. Res.* **1997**, *30*, 502−518.
(2) Albrecht, M. *Angew. Chem., Int. Ed.* **1999**, *38*, 3463−3465.
(3) Jones, C. J. *Chem. Soc. Rev.* **1998**, *27*, 289−299.
(4) Fujita, M. *Chem. Soc. Rev.* **1998**, *27*, 417−425.
(5) Batten, S. R.; Robson, R. *Angew. Chem., Int. Ed.* **1998**, *37*, 1460−1494.
(6) Constable, E. C. *Tetrahedron* **1992**, *48*, 10013−10059.
(7) Chui, S. S.-Y.; Lo, S. M.-F.; Charmant, J. P. H.; Orpen, A. G.; Williams, I. D. *Science* **1999**, *283*, 1148−1150.
(8) Kiang, Y.-H.; Gardener, G. B.; Lee, S.; Xu, Z. *J. Am. Chem. Soc.* **2000**, *122*, 6871−6883.
(9) Braga, D.; Grepioni, F. *Acc. Chem. Res.* **2000**, *33*, 601−608.
(10) Jansen, M. *Angew. Chem., Int. Ed. Engl.* **1987**, *26*, 1098−1110.
(11) Beer, P. D.; Gale, P. A. *Angew. Chem., Int. Ed.* **2001**, *40*, 486−516.
(12) Gale, P. A. *Coord. Chem. Rev.* **2001**, *213*, 79−128.
(13) Beer, P. B.; Smith, D. K. *Prog. Inorg. Chem.* **1997**, *46*, 1−96.
(14) Schmidtchen, F. P.; Berger, M. *Chem. Rev.* **1997**, *97*, 1609−1646.
(15) Lapointe, R. E.; Roof, G. R.; Abboud, K. A.; Klosin, J. *J. Am. Chem. Soc.* **2000**, *122*, 9560−9561.

10.1021/ic025935q CCC: $25.00

© 2003 American Chemical Society
Published on Web 01/10/2003

recognition, and the function of anions in supramolecular chemistry.[19−22] The features of anions such as negative charge, size, a wide range of geometries, significant solvent effects, and pH dependence imply that some anions play crucial roles in the self-assembly of functional molecules.[23−25]

Our previous results on the reactions of *n,n′*-Py$_2$Y ($n = n' = 3$ or 4; Y = O, S, Me$_2$Si) with the Ag(I) ions showed a cylindrical molecular spring via the exchange of labile anions[26−28] and a variety of coordination geometries of Ag(I) ion.[26−30] Such symmetric bipyridyl spacers have been used as molecular tectonic elements, but the exploitation of 2,4′-thiobis(pyridine) (2,4′-Py$_2$S) has until recently remained unexplored. The 2,4′-Py$_2$S is a noninnocent ligand possessing interesting N−S−N angles, potential tridentate sites, and conformational nonrigidity.[31,32] These structural properties may be useful in construction of elaborate metal compounds. Our primary purpose is to elucidate the direct roles of anions in the self-assembly of Ag(I) ion with the unique 2,4′-Py$_2$S bidirectional spacer. We describe here subtle effects and roles of polyatomic anions on the self-assembly of a series of AgX with 2,4′-Py$_2$S ($X^- = NO_3^-$, BF_4^-, ClO_4^-, PF_6^-, $CF_3CO_2^-$, and $CF_3SO_3^-$). The stable polyatomic anions have been extensively employed for the isolation of cationic transition metal skeletons.

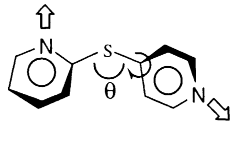

2,4′-Py$_2$S

Experimental Section

Materials and Physical Measurements. AgX and NaX ($X^- = NO_3^-$, BF_4^-, ClO_4^-, PF_6^-, $CF_3CO_2^-$, and $CF_3SO_3^-$) were purchased from Strem and Junsei Chemical Co., respectively, and were used without further purification. 2,4′-Thiobis(pyridine) (2,4′-Py$_2$S) was prepared according to the literature procedure.[31] Elemental microanalyses (C, H, N) were performed on crystalline samples by the Advanced Analysis Center at KIST using a Perkin-Elmer 2400 CHN analyzer. X-ray powder diffraction data were recorded on a Rigaku RINT/DMAX-2500 diffractometer at 40 kV and 126 mA for Cu Kα. Thermal analyses were carried out under dinitrogen atmosphere at a scan rate of 10 °C/min using a Stanton Red Croft TG 100. Infrared spectra were obtained on a Perkin-Elmer 16F PC FTIR spectrophotometer with samples prepared as KBr pellets.

General Synthetic Procedure of [Ag(2,4′-Py$_2$S)(NO$_3$)]. A methanolic solution (5 mL) of 2,4′-Py$_2$S (56 mg, 0.3 mmol) was slowly diffused into an aqueous solution (5 mL) of AgNO$_3$ (51 mg, 0.3 mmol). Colorless crystals of [Ag(2,4′-Py$_2$S)NO$_3$] suitable for X-ray crystallographic characterization formed at the interface and were obtained in 3 days in 83% yield. Anal. Calcd for $C_{10}H_8N_3O_3SAg$: C, 33.5; H, 2.3; N, 11.7. Found: C, 33.2; H, 2.2; N, 11.5. IR (KBr, cm^{-1}): $\nu(NO_3)$, 1352 (s).

[Ag$_3$(2,4′-Py$_2$S)$_4$](ClO$_4$)$_3$. Yield: 80%. Anal. Calcd for $C_{40}H_{32}N_8O_{12}S_4Cl_3Ag_3$: C, 34.9; H, 2.4; N, 8.2. Found: C, 34.6; H, 2.3; N, 8.2. IR (KBr, cm^{-1}): $\nu(ClO_4)$, 1088 (s, br).

[Ag$_3$(2,4′-Py$_2$S)$_4$](PF$_6$)$_3$. Yield: 82%. Anal. Calcd for $C_{40}H_{32}N_8F_{18}P_3S_4Ag_3$: C, 31.8; H, 2.1; N, 7.4. Found: C, 31.9; H, 2.1; N, 7.5. IR (KBr, cm^{-1}): $\nu(PF_6)$, 834 (s, br).

[Ag(2,4′-Py$_2$S)(CF$_3$CO$_2$)]. Yield: 80%. Anal. Calcd for $C_{12}H_8N_2F_3O_2SAg$: C, 35.2; H, 2.0; N, 6.8. Found: C, 36.0; H, 1.9; N, 6.8. IR (KBr, cm^{-1}): $\nu(CF_3CO_2)$, 834 (s, br).

[Ag$_3$(2,4′-Py$_2$S)$_4$](CF$_3$SO$_3$)$_3$. Yield: 81%. Anal. Calcd for $C_{43}H_{32}N_8F_9O_9S_7Ag_3$: C, 33.9; H, 2.1; N, 7.4. Found: C, 33.5; H, 2.0; N, 7.3. IR (KBr, cm^{-1}): $\nu(CF_3SO_3)$, 834 (s, br).

[Ag$_3$(2,4′-Py$_2$S)$_4$](BF$_4$)$_3$. Yield: 85%. Anal. Calcd for $C_{40}H_{32}N_8F_{12}B_3S_4Ag_3$: C, 35.9; H, 2.4; N, 8.4. Found: C, 35.5; H, 2.3; N, 8.3. IR (KBr, cm^{-1}): $\nu(BF_3)$, 1054 (s, br).

Anion Exchange of [Ag$_3$(2,4′-Py$_2$S)$_4$](ClO$_4$)$_3$ with NaPF$_6$. An aqueous solution (5 mL) of NaPF$_6$ (51 mg, 0.3 mmol) was added to an aqueous suspension (5 mL) of microcrystalline [Ag$_3$(2,4′-Py$_2$S)$_4$](ClO$_4$)$_3$ (41 mg, 0.03 mmol) at room temperature. The reaction mixture was stirred, and the precipitate was monitored after 0, 3, 6, and 24 h by IR spectra. After 24 h, the reaction mixture was filtered and washed with several aliquots of water and methanol. Elemental analysis (found: C, 32.0; H, 2.1; N, 7.6), IR, and the X-ray powder diffraction pattern are identical with those of [Ag$_3$(2,4′-Py$_2$S)$_4$](PF$_6$)$_3$ prepared by the direct reaction of AgPF$_6$ with 2,4′-Py$_2$S.

The anion exchange of the [BF_4^-] analogue with NaX ($X^- = ClO_4^-$ and PF_6^-) was carried out by the same procedure.

Crystallographic Structure Determinations. For [Ag$_3$(2,4′-Py$_2$S)$_4$](PF$_6$)$_3$ and [Ag(2,4′-Py$_2$S)(NO$_3$)], X-ray data were collected on a Bruker SMART automatic diffractometer with a graphite-monochromated Mo Kα radiation ($\lambda = 0.710\,73$ Å) and a CCD detector at ambient temperature. The 45 frames of two-dimensional diffraction images were collected and processed to obtain the cell parameters and orientation matrix. For [Ag$_3$(2,4′-Py$_2$S)$_4$](ClO$_4$)$_3$, [Ag(2,4′-Py$_2$S)(CF$_3$CO$_2$)], and [Ag$_3$(2,4′-Py$_2$S)$_4$](CF$_3$SO$_3$)$_3$, X-ray data were collected on an Enraf-Nonius CAD4 automatic diffractometer with graphite-monochromated Mo Kα ($\lambda = 0.710\,73$ Å) at ambient temperature. Unit cell dimensions were based on 25 well-centered reflections by using a least-squares procedure. During the data collection, three standard reflections monitored after every 1 h did not reveal any systematic variation in intensity. The data were corrected for Lorentz and polarization effects. Absorption effects were corrected by the empirical ψ-scan method. The structures were solved by the direct method (SHELXS 97) and

---

(16) Mason, S.; Cliford, T.; Seib, L.; Kuczera, K.; Bowman-James, K. *J. Am. Chem. Soc.* **1998**, *120*, 8899−8900.
(17) Seppelt, K. *Angew. Chem., Int. Ed. Engl.* **1993**, *32*, 1025−1027.
(18) Brown, R. A.; Pollet, P.; McKoon, E.; Eckert, C. G. Liotta, C. L.; Jessop, P. G. *J. Am. Chem. Soc.* **2001**, *123*, 1254−1255.
(19) Reed, C. A. *Acc. Chem. Res.* **1998**, *31*, 133−139.
(20) Campos-Fernandez, C. S.; Clerac, R. Dunbar, K. R. *Angew. Chem., Int. Ed.* **1999**, *38*, 3477−3479.
(21) Turner, B.; Shterenberg, A.; Kapon, M.; Suwinska, K.; Eichen, Y. *Chem. Commun.* **2001**, 13−14.
(22) Sharma, C. V. K.; Griffin, S. T.; Rogers, R. D. *Chem. Commun.* **1998**, 215−216.
(23) Withersby, M. A.; Blake, A. J.; Champness, N. R.; Hubberstey, P.; Li, W.-S.; Schröder, M. *Angew. Chem., Int. Ed. Engl.* **1997**, *36*, 2327−2329.
(24) Wu, H. P.; Janiak, C.; Rheinwald, G.; Lang, H. *J. Chem. Soc., Dalton Trans.* **1999**, 183−190.
(25) Janiak, C.; Uehlin, L.; Wu, H.-P.; Klufers, P.; Piotrowski, H.; Scharmann, T. G. *J. Chem. Soc., Dalton Trans.* **1999**, 3121−3131.
(26) Jung, O.-S.; Kim, Y. J.; Lee, Y.-A.; Park, J. K.; Chae, H. K. *J. Am. Chem. Soc.* **2000**, *122*, 9921−9925.
(27) Jung, O.-S.; Kim, Y. J.; Lee, Y.-A.; Chae, H. K.; Jang, H. G.; Hong, J. K. *Inorg. Chem.* **2001**, *40*, 2105−2110.
(28) Jung, O.-S.; Kim, Y. J.; Kim, K. M.; Lee, Y.-A. *J. Am. Chem. Soc.* **2002**, *124*, 7906−7907.
(29) Jung, O.-S.; Park, S. H.; Park, C. H.; Park, J. K. *Chem. Lett.* **1999**, 923−924.
(30) Jung, O.-S.; Park, S. H.; Lee, Y. A.; Lee, U. *Chem. Lett.* **2000**, 1012−1013.
(31) Summers, L. A. *J. Heterocycl. Chem.* **1987**, *24*, 533−544.
(32) Dunne, S. J.; Summers, L. A.; von Nagy-Felsobuki, E. I. *J. Mol. Struct.* **1992**, *268*, 373−388.

Table 1. Crystallographic Data

	$[NO_3]^a$	$[ClO_4]^b$	$[PF_6]^c$	$[CF_3CO_2]^d$	$[CF_3SO_3]^e$
formula	$C_{10}H_8N_3O_3SAg$	$C_{40}H_{32}N_8O_{12}S_4Cl_3Ag_3$	$C_{20}H_{16}N_4O_4F_9P_{1.5}S_2Ag_{1.5}$	$C_{24}H_{16}N_4F_6O_4S_2Ag_2$	$C_{43}H_{32}N_8F_9O_9S_7Ag_3$
fw	358.12	1374.97	755.75	818.27	1523.82
space group	*Pbcn*	$P\bar{1}$	*C2/c*	*C2/c*	$P\bar{1}$
a, Å	13.498(2)	8.108(2)	19.945(2)	15.894(6)	11.901(2)
b, Å	22.420(4)	10.521(2)	7.9382(6)	9.909(1)	15.473(3)
c, Å	7.994(1)	30.155(4)	32.345(2)	17.518(3)	16.855(3)
α, deg	90	91.40(1)	90	90	67.113(1)
β, deg	90	89.98(2)	97.043(2)	97.8(2)	71.465(1)
γ, deg	90	112.66(1)	90	90	84.814(2)
V, Å^3	2419.4(7)	2373.0(8)	5082.4(7)	2733(1)	2709.0(8)
Z	8	2	8	4	2
d_{calcd}, g cm^{-3}	1.966	1.924	1.975	1.989	1.868
μ, mm^{-1}	1.841	0.822	1.511	1.667	1.435
$R\ [I > 2\sigma(I)]$					
R1^f	0.0931	0.0454	0.0437	0.0355	0.0563
wR2^f	0.2556	0.1194	0.0945	0.0971	0.1443
R (all data)					
R1^f	0.1177	0.0488	0.1035	0.0501	0.0583
wR2^f	0.2798	0.1221	0.1214	0.1054	0.1463

[a] $[Ag(2,4'\text{-}Py_2S)(NO_3)]$. [b] $[Ag_3(2,4'\text{-}Py_2S)_4](ClO_4)_3$. [c] $[Ag_3(2,4'\text{-}Py_2S)_4](PF_6)_3$. [d] $[Ag(2,4'\text{-}Py_2S)(CF_3CO_2)]$. [e] $[Ag_3(2,4'\text{-}Py_2S)_4](CF_3SO_3)_3$. [f] $R1 = \sum||F_o| - |F_c||/\sum|F_o|$. [f] $wR2 = \sum w(F_o^2 - F_c^2)^2/\sum wF_o^2)^{1/2}$.

refined by full-matrix least-squares techniques (SHELXL 97).[33] The non-hydrogen atoms were refined anisotropically, and hydrogen atoms were placed in calculated positions and refined only for the isotropic thermal factors. For $[Ag_3(2,4'\text{-}Py_2S)_4](X)_3$ ($X^- = ClO_4^-$ and PF_6^-), a ClO_4^- and a PF_6^- anion, respectively, were disordered. For $[Ag(2,4'\text{-}Py_2S)(NO_3)]$, the NO_3^- anion lies in a special position. Crystal parameters and procedural information corresponding to data collection and structure refinement are given in Table 1.

Results

Construction. The slow diffusion of an organic solution of 2,4′-Py_2S into an aqueous solution of AgX ($X^- = NO_3^-$, ClO_4^-, PF_6^-, $CF_3CO_2^-$, and $CF_3SO_3^-$) afforded two kinds of products, 1:1 adducts (for NO_3^- and $CF_3CO_2^-$) and 3:4 adducts (Ag(I):2,4′-Py_2S) (for ClO_4^-, PF_6^-, and $CF_3SO_3^-$), presumably due to the coordinating nature of anions. Furthermore, each self-assembled structure is strongly dependent upon the anions (Scheme 1). The reactions of AgX ($X^- = ClO_4^-$ and PF_6^-) with 2,4′-Py_2S produce unique networks whereas treatment of AgX ($X^- = NO_3^-$ and $CF_3CO_2^-$) with 2,4′-Py_2S give anion-bridged infinite structures. The reaction of $AgCF_3SO_3$ with the same ligand affords a double strand. The molecular constructions were not significantly affected by both the change of the mole ratios and the concentrations. Moreover, when methanol or ethanol was used as solvent instead of the acetone, the same products were obtained. The solid products are insoluble in water and common organic solvents and are stable for several days even as aqueous suspensions.

Scheme 1

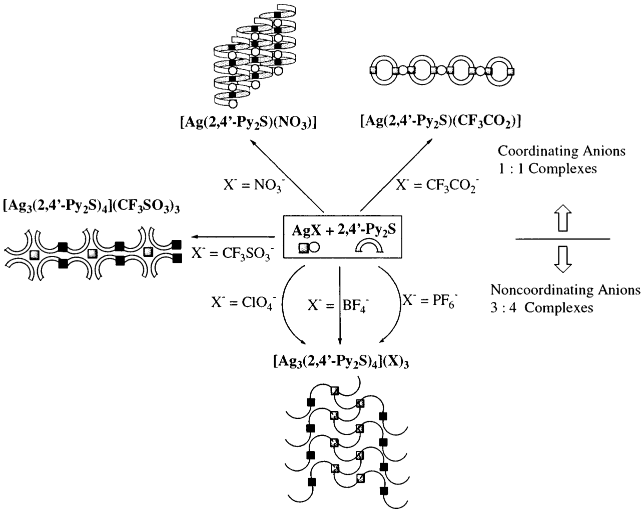

Crystal Structures. The molecular structure of $[Ag_3(2,4'\text{-}Py_2S)_4](X)_3$ ($X^- = ClO_4^-$ and PF_6^-) is depicted in Figure 1, and selected data are listed in Table 2. Their skeletal structures are the same networks consisting of Ag(I) and 2,4′-Py_2S (3:4). Each 2,4′-Py_2S spacer connects two Ag(I) ions (Ag−N = 2.162(5)−2.295(6) Å for ClO_4^-; 2.170(3)−2.268(4) Å for PF_6^-) defining the edges of 64-membered rings. The network structure seems to be sustained by the presence of face-to-face ($\pi-\pi$) stackings of pyridine rings (3.6−3.8 Å). Linear Ag(I) and trigonal Ag(I) ions exist in an 1:2 ratio in the network structure. The linear Ag(I) ion is coordinated by two 4′-Py moieties (N−Ag−N = 180. 0(4)° for ClO_4^- and 180.0(3)° for PF_6^-). The trigonal Ag(I) ion is coordinated by a 4′-Py and two 2-Py (N−Ag−N = 108.7(2)−130.3(2)° for ClO_4^-; 114.6(1)−126.1(1)° for PF_6^-). The anions do not interact with the Ag(I) ion and exist as simple counteranions (the shortest Ag(I)···X > 3.1 Å). The bond angles of C−S−C are 103.1(3)−105.1(3)° for ClO_4^- and 103.0(2)−103.1(2)° for PF_6^-, which are similar to those of 3,3′-Py_2S analogues.[27]

The structure of $[Ag(2,4'\text{-}Py_2S)(NO_3)]$ is shown in Figure 2, and selected data are listed in Table 2. Each 2,4′-Py_2S links two Ag(I) ions to give a single helix consisting of alternating Ag(I) and 2,4′-Py_2S. The nitrate anions bridge each helix in a bidentate mode (Ag−O = 2.574(5) Å). The Ag−O length is shorter than the coordinated bond (2.65(1) Å) of the tetrahedral $[Ag(3,3'\text{-}Py_2S)NO_3]$ species.[27] Thus,

---

(33) Sheldrick, G. M. *SHELXS-97: A Program for Structure Determination*; University of Göttingen: Göttingen, Germany, 1997. Sheldrick, G. M. *SHELXL-97: A Program for Structure Refinement*; University of Göttingen: Göttingen, Germany, 1997.

Table 2. Selected Bond Parameters and Structural Features

	$[NO_3]^a$	$[ClO_4]^b$	$[PF_6]^c$	$[CF_3CO_2]^d$	$[CF_3SO_3]^e$
Ag−N, Å	2.197(9)−2.213(9)	2.162(5)−2.297(6)	2.170(3)−2.268(4)	2.251(4)−2.237(5)	2.133(7)−2.425(9)
N−Ag−N, deg	153.8(3)	180.0(3)−180.0(4) 108.7(2)−130.3(2)	180.0(3) 114.6(1)−126.1(1)	148.7(2)	171.5(3)−172.6(3) 94.6(3)−135.8(2)
C−S−C, deg	103.4(4)	103.1(3)−105.1(3)	103.0(2)−103.1(2)	106.2(2)	103.1(4)−106.3(4)
Ag···X, Å	2.57			2.59−2.63	3.05
interactions, Å		$\pi-\pi = 3.6-3.8$	$\pi-\pi = 3.6-3.8$	$\pi-\pi = 3.5$	Ag−Ag = 3.226(1) $\pi-\pi = 3.5-3.7$
geometry	trigonal	linear, trigonal	linear, trigonal	square pyramid	T-shaped, T_d
motifs	helix	network	network	cyclic dimer	double strand

[a] $[Ag(2,4'\text{-}Py_2S)(NO_3)]$. [b] $[Ag_3(2,4'\text{-}Py_2S)_4](ClO_4)_3$. [c] $[Ag_3(2,4'\text{-}Py_2S)_4](PF_6)_3$. [d] $[Ag(2,4'\text{-}Py_2S)(CF_3CO_2)]$. [e] $[Ag_3(2,4'\text{-}Py_2S)_4](CF_3SO_3)_3$.

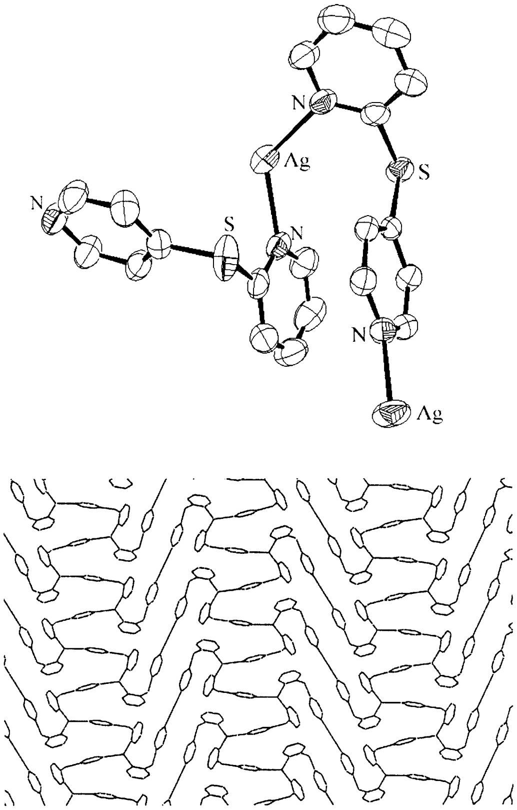

Figure 1. Asymmetric unit (top) and infinite structure (bottom) of $[Ag_3(2,4'\text{-}Py_2S)_4](ClO_4)_3$ and $[Ag_3(2,4'\text{-}Py_2S)_4](PF_6)_3$. For the infinite structure, the ClO_4^- counteranions were omitted for clarity.

the local geometry of the Ag(I) ion approximates to a trigonal arrangement (N−Ag−O = 116.2(3)°; N−Ag−N = 153.8(3)°; N−Ag−O = 86.1(3)°). The N−Ag−N angle is splayed out compared to the normal trigonal arrangement but is significantly bent from a linear arrangement owing to the presence of the coordinating anion. For the helix, there are two units in each turn (the pitch, *a* axis = 13.498(2) Å). The helical pitch is much longer than that (7.430(2) Å) of $[Ag(3,3'\text{-}Py_2O)](NO_3)$.[26] The oblong cylindrical helices are arrayed in an alternate right-handed and left-handed fashion. The C−S−C angle within the $2,4'\text{-}Py_2S$ moiety is 103.4(4)°.

The structure of $[Ag(2,4'\text{-}Py_2S)(CF_3CO_2)]$ is depicted in Figure 3, and selected data are listed in Table 2. The skeletal structure is a centrosymmetric cyclic dimer chain. The 16-membered cyclic dimer may be stabilized via a face-to-face ($\pi-\pi$) stacking of two pyridine rings (~3.5 Å). The $CF_3CO_2^-$ anion weakly links the two cyclic dimers in a tridentate fashion (Ag−O(1)′ = 2.59 Å; Ag−O(1) = 2.67 Å; Ag−O(2) = 2.63 Å). The bridged tridentate bonding mode of $CF_3CO_2^-$ anion is very rare. Thus, the local geometry of each Ag(I) ion is pseudo square pyramidal. The C−S−C angle (106.2(2)°) is relatively splayed out to sustain the cyclic dimer.

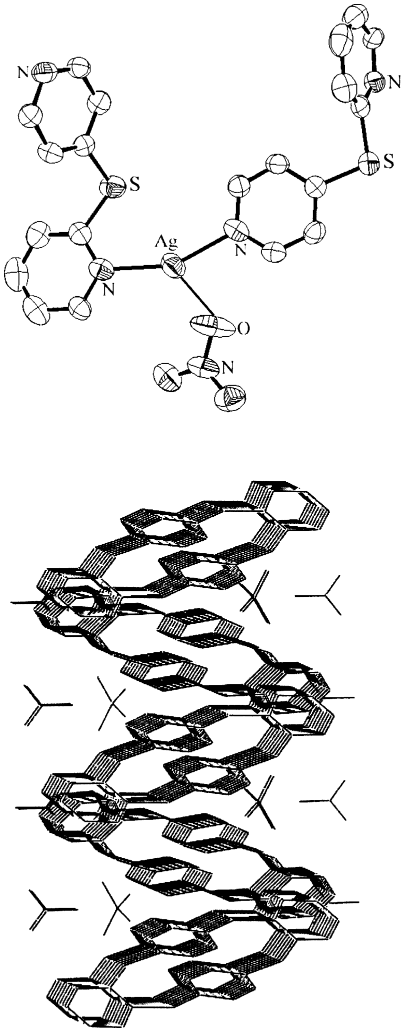

Figure 2. Asymmetric unit (top) and infinite structure (bottom) of $[Ag(2,4'\text{-}Py_2S)(NO_3)]$.

The molecular structure of $[Ag_3(2,4'\text{-}Py_2S)_4](CF_3SO_3)_3$ is depicted in Figure 4, and selected data are listed in Table 2. The skeletal structure is a unique double-strand consisting of Ag(I) and $2,4'\text{-}Py_2S$ (3:4). Each $2,4'\text{-}Py_2S$ spacer connects two Ag(I) ions (Ag−N = 2.133(7)−2.425(9) Å). The two strands interact significantly via both face-to-face ($\pi-\pi$)

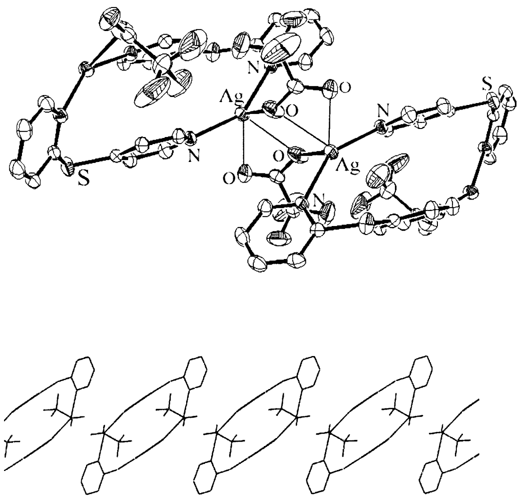

Figure 3. Asymmetric unit (top) and infinite structure (bottom) of [Ag(2,4′-Py$_2$S)(CF$_3$CO$_2$)].

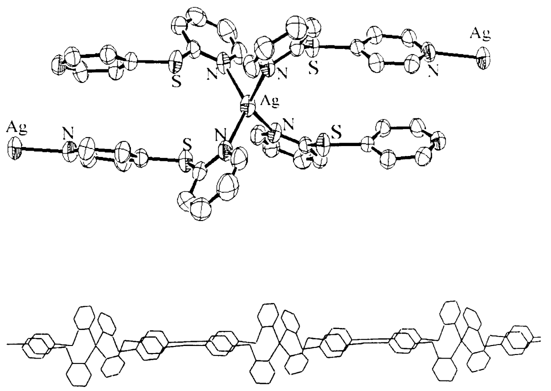

Figure 4. Asymmetric unit (top) and infinite structure (bottom) of [Ag$_3$(2,4′-Py$_2$S)$_4$](CF$_3$SO$_3$)$_3$. For the infinite structure, the CF$_3$SO$_3^-$ counteranions were omitted for clarity.

stackings of pyridine rings (3.5−3.7 Å) and strong Ag(I)···Ag(I) interactions (3.226(1) Å). The T-shaped Ag(I) ion and tetrahedral Ag(I) ion exist in a ratio of 2:1 in the crystal structure. The T-shaped Ag(I) ion is coordinated by two 4′-Py moieties (N−Ag−N = 171.5(3)−172.6(3)°) and a neighboring Ag(I) ion (N−Ag−Ag = 84.4(2)−103.7(2)°). The slightly bent angles of N−Ag−N support the presence of the Ag(I)···Ag(I) interactions. The tetrahedral Ag(I) ion is coordinated by four 2-Py moieties (N−Ag−N = 94.6(3)−135.8(2)°). The anions are positioned around the silver ions (Ag···O = 3.05 Å). The bond angles of C−S−C are in the range of 103.1(4)−106.3(4)°.

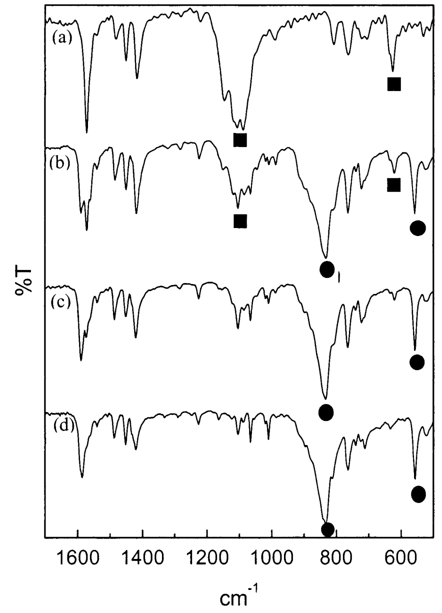

Figure 5. IR (KBr pellet) spectra during the anion exchange of [Ag$_3$(2,4′-Py$_2$S)$_4$](ClO$_4$)$_3$ with NaPF$_6$ after 0 h (a), after 3 h (b), after 6 h (c), and after 24 h (d). ■ and ● denote ClO$_4^-$ and PF$_6^-$ bands, respectively.

Anion Exchange and Thermal Stability. Anion exchange was achieved for the same network structures. The anion exchange of [Ag$_3$(2,4′-Py$_2$S)$_4$](ClO$_4$)$_3$ with PF$_6^-$ occurs smoothly in a typical aqueous media.[34,35] For [Ag$_3$(2,4′-Py$_2$S)$_4$](ClO$_4$)$_3$, the ClO$_4^-$ anions of the network exchangd completely with the octahedral PF$_6^-$ anions. The anion exchange procedure could be monitored by the characteristic IR bands of the anions. The exchange in aqueous media at room temperature was checked after 0, 3, 6, and 24 h (Figure 5). The infrared spectra show the gradual disappearance of intense ClO$_4^-$ bands (1088 cm^{-1}) and the appearance and growth of new PF$_6^-$ bands (832 cm^{-1}). The ClO$_4^-$ peaks disappear completely after 24 h. The other peaks of the spectrum remain virtually unchanged, suggesting that the skeletal structure is preserved during the anion exchange process. The elemental analysis and IR spectrum of the exchanged species are the same with those of the sample obtained by the direct reaction of AgPF$_4$ with 2,4′-Py$_2$S, indicating that the same compound is formed by the two different procedures. The X-ray powder diffraction patterns (Supporting Information) indicate that the two compounds are chemically identical. For the two exchanged samples, the high-angle peaks ($2\theta > 40°$) do not appear due to the intrinsic low crystallinity of the samples. The reverse exchange, that is, the exchange of [Ag$_3$(2,4′-Py$_2$S)$_4$](PF$_6$)$_3$ with ClO$_4^-$, occurs only slightly after 2 days. To elucidate the structure of the [BF$_4^-$] analogue indirectly, the anion exchange of the [BF$_4^-$] analogue with PF$_6^-$ was also accomplished. The elemental analysis, IR, and X-ray powder diffraction pattern of the exchanged species are identical to those of [Ag$_3$(2,4′-Py$_2$S)$_4$](PF$_6$)$_3$ prepared by the direct method, suggesting that the skeletal structure of the [BF$_4^-$] analogue is isostructural with [Ag$_3$(2,4′-Py$_2$S)$_4$](PF$_6$)$_3$. Exchange of [Ag$_3$(2,4′-Py$_2$S)$_4$](PF$_6$)$_3$ with BF$_4^-$ does not occur. The exchange of [Ag$_3$(2,4′-Py$_2$S)$_4$](ClO$_4$)$_3$ with BF$_4^-$ does not occur, but its reverse exchange occurs. The anion exchanges among the three similar skeletal structures are summarized in Scheme 2. Thus, the anion exchangeability seems to be governed by the nature of the anions[36] as well as the ionic character. Although all experiments including the preparation and anion exchange are carried out either in aqueous solutions or in aqueous suspensions, none of the compounds contain solvate water molecules. This is presum-

---

(34) Yaghi, O. M.; Li, H. *J. Am. Chem. Soc.* **1996**, *118*, 295−296.

(35) Yaghi, O. M.; Li, H.; Davies, C.; Richardson, D.; Groy, T. L. *Acc. Chem. Res.* **1998**, *31*, 474−484.

(36) Cliford, W. E.; Irving, H. *Anal. Chim. Acta* **1964**, *31*, 1−10.

Scheme 2

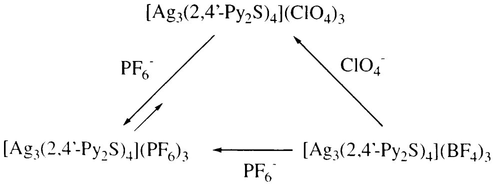

ably due to the intrinsic properties of the hydrophobic 2,4′-Py$_2$S moiety. Moreover, there are no cavities that are large enough to accommodate guest molecules such as methanol and water.

The thermal analyses have been used to establish a relationship between structure and properties.[37,38] The thermal stabilities of the present compounds are dependent upon each structure (Supporting Information). The decomposition temperatures of the 1D structures, $[Ag(2,4'\text{-}Py_2S)(CF_3CO_2)]_2$ (190 °C) and $[Ag_3(2,4'\text{-}Py_2S)_4](CF_3SO_3)_3$ (195 °C), are lower than those of the 2D structures, $[Ag_3(2,4'\text{-}Py_2S)_4](ClO_4)_3$ (230 °C) and $[Ag_3(2,4'\text{-}Py_2S)_4](PF_6)_3$ (210 °C). The $[Ag(2,4'\text{-}Py_2S)(NO_3)]$ compound decomposes at 200 °C. For $[Ag_3(2,4'\text{-}Py_2S)_4](ClO_4)_3$, the perchlorate anions appear to explode and fragment at the decomposition temperature, and thus, the perchlorate anions do not exist safely above 230 °C.

Discussion

Our intentional combinations of stable conformers of 2,4′-Py$_2$S and a variety of Ag(I) ions have formed a series of anion-dependent motifs. Each motif was efficiently constructed irrespective of the stoichiometry, the solvent type, and the concentration. First of all, why were products of two ratios (1:1 and 3:4) formed? The ClO_4^- and PF_6^- anions have been considered as common “noncoordinating” anions.[39] They have relatively little tendency to serve as ligands in the present structures. Such noncoordinating anions afford the spacer-abundant species, that is 3:4 adducts. On the other hand, the coordinating anions NO_3^- and $CF_3CO_2^-$ afford the 1:1 adducts. In the case of the noncoordinating anions, the forces used to sustain the skeletal network are the usual slipped $\pi-\pi$ interactions.[40] In contrast, the NO_3^- anion was coordinated to Ag(I) ion as shown by N−Ag(I)−N (153.8(3)°) and the Ag−O (2.574(5) Å). The coordinating NO_3^- is an obstacle to the construction of such a 2D network with $\pi-\pi$ interactions and instead induces a helical sheet via a suitable spacer conformation. The $CF_3CO_2^-$ anion was weakly bridged to the two Ag(I) ion in a tridentate manner to give the anion-bridged cyclic dimer chain. For the $CF_3SO_3^-$, the coordinating ability lies somewhere between that of the coordinating anions and the noncoordinating anions. The anion affords the 3:4 adduct like the noncoordinating anions, and the shortest $Ag(I)\cdots CF_3SO_3^-$ (3.05 Å) distance is less than the sum of the van der Waals radii (3.20 Å) of Ag and O.[41] The weak interaction seems to obstruct the formation of the 2D networks. From the Ag(I):2,4′-Py$_2$S ratios in the products and the Ag···X distances (Table 2), the coordinating nature of the anions may be ordered as $NO_3^- > CF_3CO_2^- > CF_3SO_3^- > PF_6^-$ and ClO_4^-. This order of $NO_3^- > ClO_4^-$ is consistent with the Hofmeister series that is usually given in terms of the ability of anions to stabilize the structure of macromolecules.[16] Furthermore, the present work can propose “a modified Hofmeister series” available for other polyatomic anions besides NO_3^- and ClO_4^-.

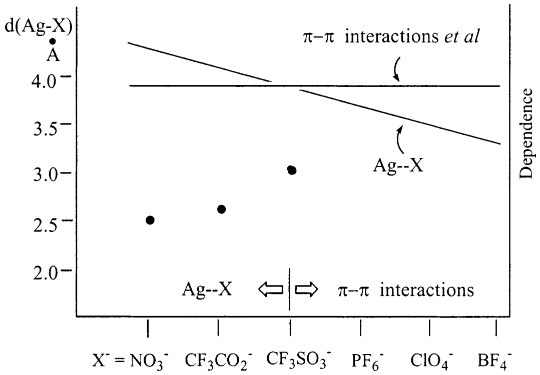

Figure 6. Correlation between the anions and $d(Ag\cdots X)$ (●).

The overall motifs including the local geometry and mole ratios of the products appear to be delicately associated with the nature of anions. The slipped $\pi-\pi$ interactions and the Ag···X interactions are competitive in constructing the present molecular structures. This study examines on the change in Ag···X interactions relative to the constant $\pi-\pi$ interactions of the 2,4′-Py$_2$S. These features may be schematically summarized in terms of a relative competition (presented by an arbitrary slope) between Ag···X interactions and $\pi-\pi$ interactions in the self-assembly of Ag(I) compounds as shown in Figure 6.

To the right of the crossing point ($CF_3SO_3^-$), the Ag···X interactions gradually weaken and the $\pi-\pi$ interactions are more significant.[40] To the left of the crossing point, the Ag···X interactions play an important role in the molecular construction. Since it forms a compound isostructural to $[Ag_3(2,4'\text{-}Py_2S)_4](ClO_4)_3$, the BF_4^- anion can be categorized in noncoordinating class such as PF_6^- and ClO_4^-. Since the anion exchangeability is related to anion binding,[12] the coordinating order of PF_6^-, ClO_4^-, and BF_4^- anions was determined by anion exchange. That is, $[Ag_3(2,4'\text{-}Py_2S)_4](ClO_4)_3$ was easily exchanged by PF_6^-. Furthermore, the anion exchange of the $[Ag_3(2,4'\text{-}Py_2S)_4](BF_4)_3$ analogue with PF_6^- was accomplished, but the exchange of the $[Ag_3(2,4'\text{-}Py_2S)_4](PF_6)_3$ analogue with ClO_4^- or BF_4^- was limited. The anion exchange properties show that the coordinating nature of the anions is in the order $PF_6^- > ClO_4^- > BF_4^-$. The coordinating nature is consistent with the order of association constants.[42] Thus, the coordinating nature of all anions can be summarized in the order $NO_3^- > CF_3CO_2^- > CF_3SO_3^-$

---

(37) Jung, O.-S.; Park, S. H.; Kim, D. C.; Kim, K. M. *Inorg. Chem.* **1998**, *37*, 610−611.

(38) Jung, O.-S.; Park, S. H.; Kim, K. M.; Jang, H. G. *Inorg. Chem.* **1998**, *37*, 5781−5785.

(39) Chew, K. F.; Healy, M. A.; Khalil, M. I.; Logan, N.; Derbyshire, W. *J. Chem. Soc., Dalton Trans.* **1975**, 1315−1358.

(40) Janiak, C. *J. Chem. Soc., Dalton Trans.* **2000**, 3885−3896.

(41) Huheey, J. E. *Inorganic Chemistry, Principles of Structure and Reactivity*, 2nd ed.; Harper & Row: New York, 1978; pp 230−236.

(42) Schnebeck, R.-D.; Freisinger, E.; Lippert, B. *Angew. Chem., Int. Ed.* **1999**, *38*, 168−171.

> PF_6^- > ClO_4^- > BF_4^-. The weak nucleophilicity and strong electron-withdrawing nature of fluorine atom as well as Lewis acidic character of the boron atom may be major factors contributing to the least coordinating ability of BF_4^-.

Conclusions

The first metal complexes of 2,4′-Py_2S demonstrate that the spacer is a fascinating tectonic unit without any particular strain in the construction of variable skeletons. The nonrigid 2,4′-Py_2S spacer is responsive to the nature of anions. A new coordinating series of polyatomic anions has been quantitatively determined via the structural analyses and the anion exchanges. The anion series can be extended as a crucial factor for the design and development of metal-based desirable materials such as anion sensors, molecular control,[43] ion exchangers, chemical delivery, and intercalators.

Acknowledgment. This work was supported in part by the Ministry of Science and Technology in Korea.

Supporting Information Available: Crystallographic data for [Ag(2,4′-Py_2S)(NO_3)], [Ag_3(2,4′-Py_2S)$_4$](ClO_4)$_3$, [Ag_3(2,4′-Py_2S)$_4$](PF_6)$_3$, [Ag(2,4′-Py_2S)(CF_3CO_2)], and [Ag_3(2,4′-Py_2S)$_4$](CF_3SO_3)$_3$, IR spectra and X-ray powder diffraction patterns of [Ag_3(2,4′-Py_2S)$_4$](PF_6)$_3$ prepared by the anion exchange of [Ag_3(2,4′-Py_2S)$_4$](BF_4)$_3$ with PF_6^-, and TGA traces of [Ag(2,4′-Py_2S)(NO_3)], [Ag_3(2,4′-Py_2S)$_4$](ClO_4)$_3$, [Ag_3(2,4′-Py_2S)$_4$](PF_6)$_3$, [Ag(2,4′-Py_2S)(CF_3CO_2)], and [Ag_3(2,4′-Py_2S)$_4$](CF_3SO_3)$_3$. This information is available free of charge via the Internet at http://pubs.acs.org.

IC025935Q

---

(43) Lee, Y.-A.; Jung, O.-S. *Angew. Chem., Int. Ed.* **2001**, *40*, 3868−3870.